



Dual-layer dual-energy CT for characterization of adrenal nodules: can virtual unenhanced images replace true unenhanced acquisitions?

Jinjin Cao¹ · Simon Lennartz^{1,2} · Anushri Parakh¹ · Evita Joseph¹ · Michael Blake¹ · Dushyant Sahani³ · Avinash Kambadakone¹

Received: 1 January 2021 / Revised: 6 March 2021 / Accepted: 10 March 2021 / Published online: 8 April 2021
© The Author(s), under exclusive licence to Springer Science+Business Media, LLC, part of Springer Nature 2021

Abstract

Purpose To investigate the diagnostic performance of dual-layer dual-energy CT (dIDECT) in the evaluation of adrenal nodules.

Methods In this retrospective study, 66 patients with triphasic dIDECT (unenhanced, venous phase (VP), delayed phase (DP)) for suspected adrenal lesions were included. Virtual unenhanced images (VUE) were derived from VP acquisitions. Reference diagnoses were established with true unenhanced (TUE) attenuation, absolute washout, follow-up imaging and pathological data. Attenuation for adrenal lesions and abdominal tissues was acquired on TUE, VUE, VP and DP images. VUE and TUE attenuation were compared in all included tissues. Characterization of adrenal nodules based on TUE and VUE attenuation was investigated. ROC analysis was used to determine an adjusted threshold for diagnosing lipid-rich adenomas.

Results Seventy-three adrenal nodules (mean size: 18.9 ± 8.9 mm) were identified in 66 patients (38 females, 28 males; age: 61 ± 13 years) including adenoma ($n=65$), metastases ($n=2$), pheochromocytoma ($n=3$), adrenocortical carcinoma ($n=1$) and myelolipoma ($n=2$). Mean attenuation of all included tissues except for the abdominal aorta ($p=0.11$) was significantly higher in VUE compared to TUE images, including the attenuation of adrenal nodules (20.0 ± 17.2 vs. 7.1 ± 19.8 ; $p < 0.05$). Classification of adrenal adenomas as lipid-rich based on VUE attenuation ≤ 10 HU yielded a sensitivity/specificity of 0.2/1.0, while an adjusted threshold of ≤ 22 HU yielded a sensitivity/specificity of 0.82/0.85.

Conclusion dIDECT-derived VUE images overestimated attenuation in adrenal nodules, resulting in low sensitivity for diagnosis of lipid-rich adenomas using the established 10 HU threshold. Based on an adjusted threshold (≤ 22 HU) a higher sensitivity was attained, yet at the expense of a lower specificity, warranting further validation.

Keywords Dual-energy CT · Adrenal nodules · Virtual unenhanced images · Lesion characterization · Adrenal glands

Abbreviations

DECT Dual-energy CT

dIDECT Dual-layer dual-energy CT

DP Delayed phase

TUE True unenhanced images

VP Venous phase

VUE Virtual unenhanced images

Jinjin Cao and Simon Lennartz are Co-first authors who contributed equally.

✉ Avinash Kambadakone
akambadakone@mgh.harvard.edu

¹ Department of Radiology, Harvard Medical School, Massachusetts General Hospital, 55 Fruit Street, White 270, Boston, MA 02114-2696, USA

² Institute for Diagnostic and Interventional Radiology, Faculty of Medicine and University Hospital Cologne, University of Cologne, Kerpener Straße 62, 50937 Cologne, Germany

³ Department of Radiology, University of Washington, UWMC Radiology RR218, 1959 NE Pacific St, Seattle, WA 98195, USA

Introduction

Incidental adrenal nodules are detected in 4% of abdominal computed tomography (CT) scans [1]. Most of these lesions are benign adrenal adenomas, even in oncologic patients [2]. However, single-phase contrast-enhanced CT is limited in the diagnosis and characterization of adrenal lesions, often necessitating additional testing when adrenal nodules are detected incidentally. A dedicated multiphasic adrenal mass protocol contrast-enhanced CT is widely accepted and used to characterize adrenal nodules and in particular to identify

adrenal adenomas. This usually comprises acquisition of an unenhanced image, an early contrast-enhanced phase and a delayed phase 10–15 min after contrast media injection. An unenhanced CT allows for the identification of lipid-rich adenomas as these nodules demonstrate a low pre-contrast CT attenuation due to the presence of rich intracytoplasmic lipid content. An adrenal lesion that is 10 HU or less is classified as a lipid-rich adenoma (sensitivity 71%; specificity 98%) [3–7]. By contrast, lipid-poor adenomas with attenuation higher than 10 HU can be characterized as such by calculation of absolute washout values from early and delayed phase image acquisitions with an absolute washout greater than 60% being highly suggestive for adenoma [2, 8–10].

Dual-energy CT (DECT) allows for the generation of virtual unenhanced (VUE) images by means of material decomposition. Such VUE images have been investigated for their capability in adrenal lesion characterization, yet almost all of prior adrenal DECT research was performed on emission based dual-source or rapid kV switching DECT systems. One of the key advantages of VUE images is the possibility to considerably reduce radiation dose by elimination of the unenhanced CT scans [11–16]. However, some studies pointed out that VUE images might overestimate attenuation values compared to true TUE acquisitions [17, 18].

The dual-layer DECT (dIDECT) is based on a detector with a stacked scintillator in which high and low energies are recorded separately [19]. A previous study suggested that the different technical approaches to DECT might result in differences regarding material quantification which is why further investigation of dIDECT-based adenoma lesion

characterization is needed [20]. The purpose of this study was therefore to investigate, if VUE images derived from dIDECT can be used to classify adrenal nodules based on established quantitative criteria and to determine adjusted thresholds for dIDECT-derived VUE, if necessary.

Methods

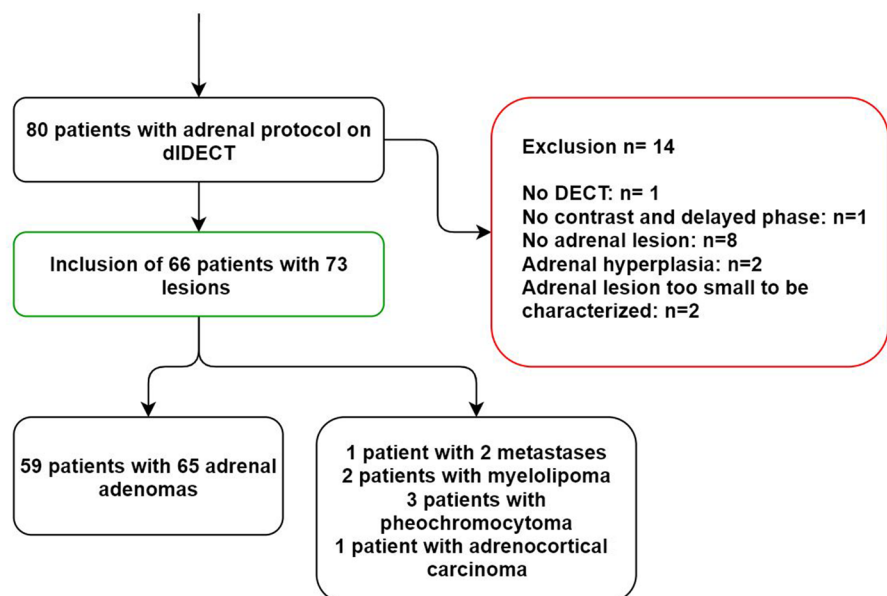
This retrospective study was approved by our institutional review board and the requirement for written informed consent was waived. The picture archiving and communication system (PACS; Visage 7, Visage Imaging, San Diego, CA) was screened to identify patients ≥ 18 years who underwent dedicated tri-phasic adrenal protocol CT for characterization of incidental adrenal nodules on a dIDECT scanner over a 26-month period (July 2018–September 2020). This initial search yielded 80 patients with adrenal protocol dIDECT, from which 14 were excluded (Fig. 1). The final cohort included 66 consecutive patients (38 female, 28 male; mean age: 61 ± 13 years; mean weight: 84 ± 19 kg). Detailed patient information was recorded from the medical records to document patient demographics, endocrine work up details, treatment details, surgical and pathology reports for establishing reference diagnoses.

CT technique

All the patients in this study underwent an adrenal protocol CT on a dIDECT (iQon, Philips Healthcare, Best, The Netherlands). All scans were conducted in supine position with an

Fig. 1 Study flowchart for inclusion and exclusion of patients

Initial database screening July 2018–September 2020



initial unenhanced acquisition (TUE) followed by scanning in the portal venous phase (VP; delay: 75 s) and delayed phase (DP; delay: 15 min). Scan parameters were as follows: tube voltage 120 kVp, tube current modulation: on (3D DOM, Philips Healthcare), collimation: 64×0.625 , matrix size: 512×512 ; gantry revolution time (0.35 ± 0.14 s) and pitch (1.2 ± 0.09) were adjusted automatically for each examination. Patients received a body weight adapted injection of iodinated contrast media (Isovue 370 mg/mL, Bracco Diagnostics, Princeton, NJ, USA). Injection parameters were as follows: under 200 lbs: 90 mL at a flow rate of 2.5–3.0 mL/s; over 201 lbs: 120 mL at 3 mL/s. Both weight groups received a saline chaser of 40 mL at an injection rate of 3 mL/second.

Image reconstruction

Axial images with a slice thickness and section increment of 2.5 mm were reconstructed from the TUE, VP and DP acquisitions using a hybrid iterative reconstruction algorithm (iDose 3, Philips Healthcare). VUE images derived from venous phase acquisitions were reconstructed with a 2.5 mm slice thickness as well (Spectral, Filter B, Philips Healthcare). CT dose index (CTDI) was recorded for each phase.

Quantitative analysis

A radiologist with 12 years of experience in abdominal CT assessment who was blinded to the final diagnosis quantified the attenuation of adrenal lesions, abdominal aorta, erector spinae muscle, extra-abdominal subcutaneous fat, main portal vein and liver parenchyma on TUE, VUE, PV and DP images. Each tissue was measured by placing 3 circular regions of interest (ROI) within it. For the adrenal lesions, the ROIs were placed at the level of the largest lesion diameter as well as on the adjacent slices above and below that level. All ROIs were drawn as large as possible, yet as to remain within lesion boundaries and avoid inclusion of unrepresentative tissue such as calcifications, blood vessels and evident necrosis. The adrenal ROI size ranged between 0.22 and 2.8 cm².

Reference standard

All adrenal adenomas included in the final analysis had to be unequivocally diagnosed as such by TUE attenuation ≤ 10 HU or an absolute washout calculated with VP, DP and TUE images of $> 60\%$ as follows:

$$\text{Washout (TUE)} = \frac{\text{HU[VP]} - \text{HU[DP]}}{\text{HU[VP]} - \text{HU[TUE]}} \times 100$$

All adenomas that were included were unequivocally diagnosed as such on CT either with TUE attenuation or washout and lesion stability over a 6-month period as well as

in- and out-of-phase MR characteristics served as additional confirmation. For 19 patients, follow-up was available (CT: $n = 17$ patients, MR: $n = 2$ patients). 48 patients had prior imaging (CT: $n = 41$, MR: $n = 6$, PET/CT: $n = 1$).

Based on the final reference standard, 65 adrenal adenomas (45 lipid-rich adenomas, 20 lipid-poor adenomas) and 8 non-adenomas ($n = 2$ adrenal metastases, $n = 1$ adrenocortical carcinoma, $n = 3$ pheochromocytoma, $n = 2$ myelolipoma) were included. However, while all adrenal lesions were included for testing the agreement between TUE and VUE images in general, the 2 myelolipomas were excluded in the classification as they would have led to false positive quantitative determination of lipid-rich adenoma that would not have happened clinically as they could be easily be diagnosed visually due to intralesional macroscopic fat. Diagnoses of all other non-adenomas that were included in the classification analysis were pathologically confirmed. Pathological tissue was obtained either using CT guided biopsy (for $n = 2$ metastases) or surgical resection (for $n = 3$ pheochromocytoma, and one adrenocortical carcinoma).

Figure 2 displays representative cases for lipid-rich and lipid-poor adenoma

Classification of lipid-rich adrenal adenoma based on VUE attenuation

Using the above-mentioned reference standard, diagnostic performance of VUE images at adrenal nodule classification was evaluated as follows:

For detection of lipid-rich adenomas, sensitivity of VUE using the established attenuation threshold of ≤ 10 HU was evaluated. In addition, a receiver operating characteristics (ROC) analysis was performed to determine the optimal VUE threshold for detection of lipid-rich adenomas. To evaluate overall adrenal nodule classification based on VUE, the sensitivity and specificity for identifying lipid-rich adenomas ($n = 45$) amongst adrenal nodules included in the classification analysis ($n = 71$) was calculated.

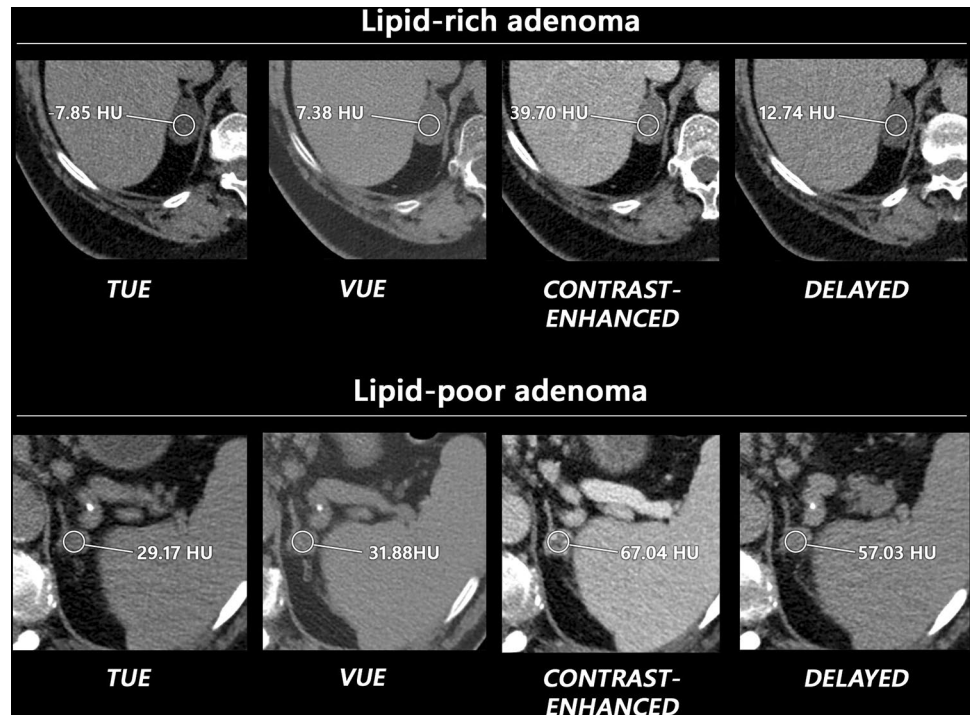
Agreement between attenuation obtained from virtual and true unenhanced images

To more broadly evaluate quantitative agreement between VUE and TUE images, mean attenuation values were compared for all included tissues (i.e. all adrenal lesions irrespective of lesion type, liver, abdominal aorta, portal vein, erector spinae muscle, subcutaneous fat).

Statistical analysis

Statistical analyses were performed with JMP software (Version 14, SAS). Continuous variables are indicated as mean \pm standard deviation and categorical variables

Fig. 2 Lipid-rich and lipid-poor adenomas. Top row: Axial true unenhanced (TUE), virtual unenhanced (VUE), contrast-enhanced, and delayed phase dual-energy CT images in a 63-year-old woman with adrenal lipid-rich adenoma, respectively. Bottom row: Axial true unenhanced (TUE), virtual unenhanced (VUE), contrast-enhanced, delayed phase dual-energy CT images in a 55-year-old man with adrenal lipid-poor adenoma, respectively. Relevant overestimation of VUE can be appreciated in the lipid-rich adenoma



are written as frequencies or percentages. Following non-normal distribution determined with Shapiro–Wilk-test, attenuation derived from VUE and TUE images were compared using the non-parametric Wilcoxon signed rank test. Receiver operating characteristics (ROC) analysis with Youden’s J method was used to determine the optimal adjusted threshold for diagnosis of lipid-rich adenoma based on VUE attenuation. A *p* value below 0.05 was considered statistically significant.

Results

Demographics

Seventy-three adrenal nodules were included in 66 patients (38 female, 28 male; 61 ± 13 years) including 59 patients with 65 adrenal adenomas (45 defined as lipid-rich as per TUE attenuation ≤ 10 HU), one patient with 2 metastases, 2 patients with myelolipomas, 3 patients with pheochromocytomas and one patient with adrenocortical carcinoma. The follow-up period ranged from 5.5 to 18 months (11 ± 4 months). Detailed information on diagnoses are given in Table 1.

Table 1 Patient and adrenal nodule characteristics

	Patients	Lesions	Gender (F/M)	Weight (kg)	Age (years)
All adrenal nodules	66	73	38/28	83.6 ± 19.2	61.0 ± 13.0
Adrenal adenoma	59	65	35/24	84.1 ± 19.3	61.7 ± 13.1
Lipid-rich adenoma	41	45	23/18	80.8 ± 21.1	59.9 ± 12.5
Lipid poor adenoma	18	20	11/7	82.5 ± 16.2	65.0 ± 10.8
Non-adenoma	7	8	4/3	79.3 ± 20.6	54.0 ± 13.0
Adrenal metastases	1	2	F	85.3	78
Pheochromocytoma	3	3	2/1	74.4 ± 21.4	55.8 ± 13
Adrenocortical carcinoma	1	1	F	76.2	22
Myelolipoma	2	2	1/1	85.1 ± 17	55 ± 13.8

*Myelolipomas were only included in the comparison of VUE and TUE attenuation and were not included in the classification of lipid-rich adenomas based on HU attenuation in VUE and TUE images

Classification of lipid-rich adrenal adenoma based on VUE attenuation

The sensitivity/specificity of VUE using the established attenuation threshold of ≤ 10 HU for identifying lipid-rich adenomas was 0.2 (9/45)/1.0 (26/26). ROC analysis using the Youden's J method revealed the optimal adjusted VUE attenuation threshold to be 22 HU, yielding a sensitivity and specificity of 0.82 (37/45)/0.85 (22/26) for diagnosis of lipid-rich adrenal adenoma (Table 2).

Agreement between attenuation obtained from virtual and true unenhanced images

There were significant differences between the mean attenuation values on VUE and TUE images for all adrenal lesions, adrenal adenomas, the liver, portal vein, erector spinae muscle and fat (all $p < 0.05$). The only tissue without significant differences between mean attenuation on TUE and VUE images was the aorta ($p = 0.11$). Table 3 and Fig. 3 provide a detailed overview on mean attenuation values for all included tissues. Mean lesion size of all adrenal lesions was 18.9 ± 8.9 mm.

The mean differences between VUE and TUE were highest for adrenal lesions: 13.5 ± 8.9 HU for adenomas and 12.8 ± 9.0 HU for all adrenal lesions. In other tissues, the

differences were 6.3 ± 4.9 HU for the liver, 1.4 ± 6.4 HU for the aorta, 2.8 ± 6.1 HU for the portal vein, 4.9 ± 3.7 HU for the erector spinae muscle and 8.2 ± 5.1 HU for fat (Fig. 4). The differences between VUE and TUE attenuation was within a range of -10 to $+10$ HU [21] in 24/73 (32.88%) of measurements of all adrenal lesions, in 19/65 of adrenal adenomas (29.2%), in 57/66 (86.4%) of patients for the aorta, in 60/66 (86.4%) of patients for the muscle, in 44/66 (66.7%) of patients for the fat, in 59/66 (89.4%) of patients for the portal vein and in 52/66 (78.8%) of patients for the liver. Disagreement between VUE and TUE outside of the 10 HU range was almost entirely caused by overestimation of attenuation in VUE images (107 measurements with TUE/VUE disagreement, 102 by overestimation (i.e. VUE-TUE > 10 HU), 5 by underestimation (i.e. VUE-TUE < -10 HU).

Radiation dose

Mean CTDI was 12.3 ± 6.9 mGy for the TUE acquisition, 12.4 ± 6.9 mGy for the VP acquisition and 12.4 ± 6.9 mGy for the DP acquisition, yielding a potential dose saving of 33% in case of replacement of TUE by VUE.

Discussion

In our study, we found an overestimation of attenuation values of adrenal nodules on VUE images and all further examined tissues except for the abdominal aorta. For 49 of 73 adrenal lesions included, the overestimation was greater than 10 HU. Consequently, the sensitivity of VUE images for diagnosing lipid-rich adenomas using the established 10 HU threshold was low (sensitivity/specificity: 0.2/1.0). By means of ROC analysis, the optimal VUE attenuation threshold for identifying lipid-rich adenomas was calculated to be 22 HU, yielding a sensitivity/specificity of 0.82/0.85.

VUE images have been investigated with regards to their suitability for replacing TUE image acquisitions for adrenal nodule classification, which would allow for considerable

Table 2 Attenuation cut-offs for diagnosis of lipid-rich adenomas

	VUE attenuation ≤ 10 HU ^a	VUE attenuation ≤ 22 HU ^b
Sensitivity	0.20 (9/45)	0.82 (37/45)
Specificity	1.00 (26/26)	0.85 (22/26)

Diagnosis of lipid-rich adenomas ($n = 45$) amongst all adrenal lesions ($n = 71$) using virtual unenhanced attenuation.

^aThe results displayed are using the established 10 HU threshold

^bThe results displayed are using a proposed threshold of 22 HU which provided optimal diagnostic performance in the ROC analysis

Table 3 Attenuation values of abdominal structures on VUE and TUE

	TUE	VUE	<i>p</i> -value VUE vs. TUE	Portal venous phase	Delayed phase
Adenomas	6.9 ± 12.8	20.5 ± 9.9	< 0.0001	61.6 ± 21.3	23.8 ± 15
All adrenal lesions	7.1 ± 19.8	20 ± 17.2	< 0.0001	61.1 ± 29.2	24.1 ± 21.2
Aorta	42.3 ± 4.5	43.7 ± 4.6	0.11	158.5 ± 34	79 ± 8.4
Fat	-104 ± 10.9	-95.8 ± 12.4	< 0.0001	-100.8 ± 12.9	-95.3 ± 19.6
Liver	51.9 ± 11.6	58.2 ± 9.1	< 0.0001	104.6 ± 19.6	65.8 ± 15.8
Muscle	42.6 ± 7	47.5 ± 5.8	< 0.0001	52.4 ± 7.2	52.8 ± 12.9
Portal vein	40.7 ± 5.4	43.5 ± 4.5	0.0002	171.1 ± 18.6	72.3 ± 13.7

TUE true unenhanced, VUE virtual unenhanced

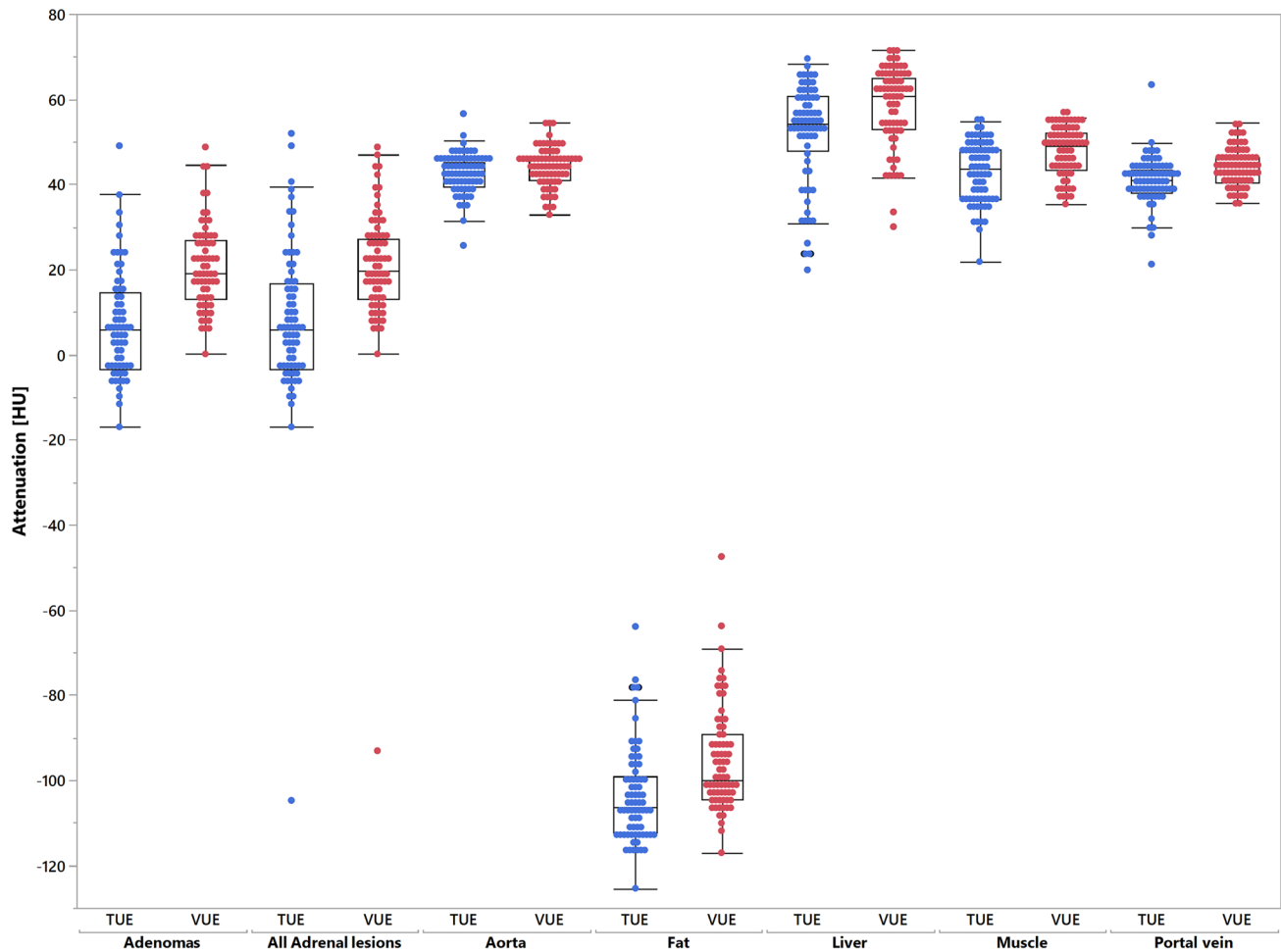


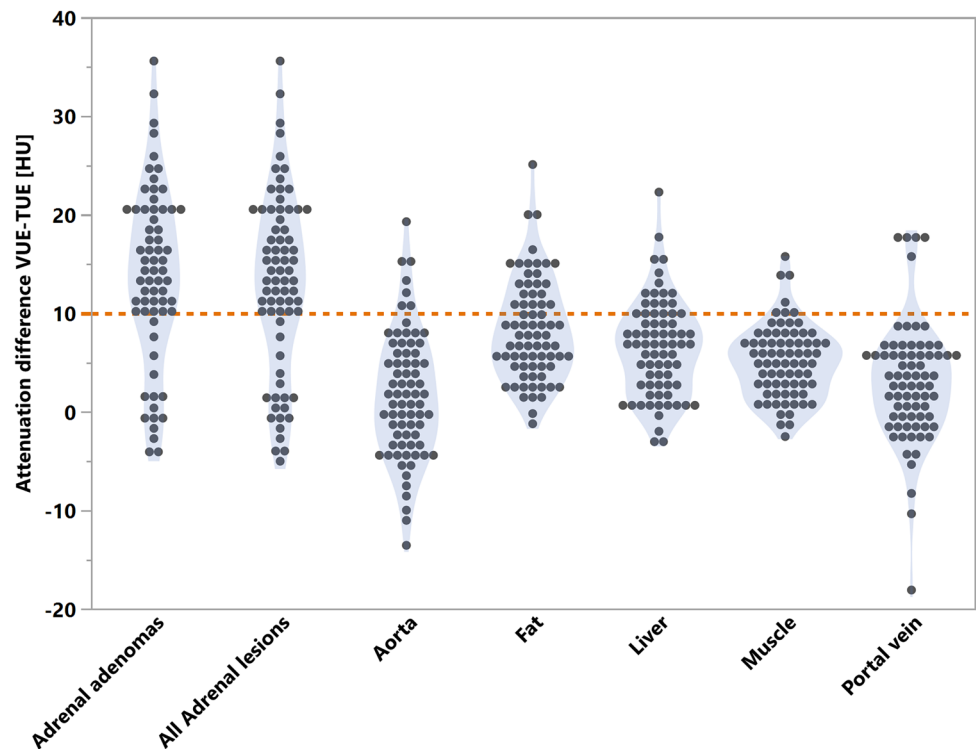
Fig. 3 Attenuation value plot between TUE and VUE on adenomas, all adrenal lesions, aorta, fat, liver, erector spinae, portal vein

reduction of radiation dose and follow-up exams in case nodules are detected incidentally. While many studies have shown promising results in this regard, others described a systematic overestimation of attenuation in VUE images [11, 22]. For the dIDECT, a detector based DECT approach which has been introduced relatively recently, there is limited evidence for adrenal nodule classification based on VUE images.

Our findings are in line with a recently published study, in which a systematic overestimation of attenuation in VUE images derived from dIDECT was described for adrenal adenoma diagnosis [18]. While Nagayama et al. used a combination of VUE images and iodine maps to mitigate this problem at differentiation of adrenal adenomas and metastases, we were able to show that adjusting the VUE attenuation threshold yielded an adequate diagnostic accuracy for identifying lipid-rich adenomas. However, it must be noted that the proposed higher threshold decreased specificity which is why this threshold corrected for VUE overestimation should be critically validated

before clinical application. Compared to a dual-source DECT-based study by Helck et al., which found a sensitivity/specificity of 0.73/1.0 for a 10 HU threshold in VUE images [22], the diagnostic performance we found for this established threshold in VUE images was very low (0.2/1.0) which is well explained by our observation that VUE overestimation was highest in adrenal adenomas. Adenomas characteristically contain intracytoplasmic fat along with soft tissue components and demonstrate iodine enhancement—one possible explanation for the overestimation could therefore be that the dIDECT-derived two material decomposition algorithm might be impacted in terms of accuracy by the presence of a third material. Interestingly, Ananthkrishnan et al. previously reported that the bias between VUE and TUE attenuation was highest within fat [23]. Another explanation could be the relatively high spectral overlap in dIDECT compared to other scanner types [19]. In another study investigating dIDECT-derived VUE images for differentiation of adrenal adenomas and metastases, Laukamp et al. found a low

Fig. 4 Attenuation value difference between TUE and VUE on adenomas, all adrenal lesions, aorta, fat, liver, erector spinae, portal vein



sensitivity/specificity of 0.48/1.0 when applying the 10 HU threshold, which was improved to 0.96/1.0 when raising the threshold to 20 HU [24]. While the low sensitivity they found is in line with our findings, the equally high specificity they reported could be due to the limited number of adenomas included in their study ($n = 23$).

Our study has limitations that should be acknowledged. First, it was a retrospective study performed at one institution. Second, most lesions that were included were diagnosed based on currently accepted imaging and clinical criteria rather than histopathologic workup. Third, the number of lesions, particularly that of non-adenomatous nodules, is small, which is why our results should be confirmed in a larger-scale investigation. Fourth, the proposed adjusted VUE threshold we derived from our study data should be tested in an independent cohort before being applied clinically. Last, the results we found only apply to the DECT technology we investigated i.e. dIDECT. It is known that there is a certain degree of inter-scanner variability which limits generalizability of the results we found to other DECT scanner types.

To conclude, virtual unenhanced images derived from detector based dual-layer dual-energy CT overestimated attenuation in the assessment of adrenal nodules, resulting in a limited sensitivity for the established 10 HU attenuation threshold. We propose an adjusted virtual unenhanced attenuation threshold of 22 HU for identifying lipid-rich

adenomas which should be validated in future large cohort studies.

Funding This study was funded by Philips (Grant number 2018A006560 to Avinash Kambadakone) and the Deutsche Forschungsgemeinschaft (DFG, German Research Foundation)—LE 4401/1-1 to Simon Lennartz (Project number 426969820)

Declarations

Disclosures Avinash Kambadakone: Research grants (GE and Philips Healthcare). Simon Lennartz: Research support (Philips Healthcare).

References

1. Bovio S, Cataldi A, Reimondo G, et al. (2006) Prevalence of adrenal incidentaloma in a contemporary computerized tomography series. *J Endocrinol Invest* 29(4):298–302
2. Caoili EM, Korobkin M, Francis IR, et al. (2002) Adrenal masses: characterization with combined unenhanced and delayed enhanced CT. *Radiology* 222(3):629–633
3. Lee MJ, Hahn PF, Papanicolaou N, et al. (1991) Benign and malignant adrenal masses: CT distinction with attenuation coefficients, size, and observer analysis. *Radiology* 179(2):415–418
4. Boland GW, Lee MJ, Gazelle GS, et al. (1998) Characterization of adrenal masses using unenhanced CT: an analysis of the CT literature. *AJR Am J Roentgenol* 171(1):201–204
5. Blake MA, Cronin CG, Boland GW (2010) Adrenal imaging. *AJR Am J Roentgenol* 194(6):1450–1460

6. Yip L, Tublin ME, Falcone JA, Nordman CR, et al. (2010) The adrenal mass: correlation of histopathology with imaging. *Ann Surg Oncol* 17(3):846–852
7. Legmann P (2009) Adrenal incidentaloma: management approaches: CT - MRI. *J Radiol* 90(3 Pt 2):426–443
8. Peña CS, Boland GW, Hahn PF, et al. (2000) Characterization of indeterminate (lipid-poor) adrenal masses: use of washout characteristics at contrast-enhanced CT. *Radiology* 217(3):798–802
9. Park BK, Kim CK, Kim B, et al. (2007) Comparison of delayed enhanced CT and chemical shift MR for evaluating hyperattenuating incidental adrenal masses. *Radiology* 243(3):760–765
10. Caoili EM, Korobkin M, Francis IR, et al. (2000) Delayed enhanced CT of lipid-poor adrenal adenomas. *AJR Am J Roentgenol* 175(5):1411–1415
11. Kim YK, Park BK, Kim CK, et al. (2013) Adenoma Characterization: Adrenal Protocol With Dual-Energy CT. *Radiology* 267(1):155–163
12. Graser A, Johnson TR, Chandarana H, et al. (2009) Dual energy CT: preliminary observations and potential clinical applications in the abdomen. *Eur Radiol* 19(1):13–23
13. Graser A, Johnson TR, Hecht EM, et al. (2009) Dual-energy CT in patients suspected of having renal masses: can virtual non-enhanced images replace true nonenhanced images? *Radiology* 252(2):433–440
14. Graser A, Becker CR, Staehler M, et al. (2010) Single-phase dual-energy CT allows for characterization of renal masses as benign or malignant. *Invest Radiol* 45(7):399–405
15. Neville AM, Gupta RT, Miller CM, et al. (2011) Detection of renal lesion enhancement with dual-energy multidetector CT. *Radiology* 259(1):173–183
16. Gupta RT, Ho LM, Marin D, et al. (2010) Dual-energy CT for characterization of adrenal nodules: initial experience. *AJR Am J Roentgenol* 194(6):1479–1483
17. Botsikas D, Triponez F, Boudabbous S, et al. (2014) Incidental adrenal lesions detected on enhanced abdominal dual-energy CT: can the diagnostic workup be shortened by the implementation of virtual unenhanced images? *Eur J Radiol*. 83(10):1746–1751
18. Nagayama Y, Inoue T, Oda S, et al. (2020) Adrenal Adenomas versus Metastases: Diagnostic Performance of Dual-Energy Spectral CT Virtual Noncontrast Imaging and Iodine Maps. *Radiology* 296(2):324–332
19. McCollough CH, Leng S, Yu L, et al. (2015) Dual- and Multi-Energy CT: Principles, Technical Approaches, and Clinical Applications. *Radiology* 276(3):637–653
20. Jacobsen MC, Schellingerhout D, Wood CA, et al. (2018) Intermanufacturer Comparison of Dual-Energy CT Iodine Quantification and Monochromatic Attenuation: A Phantom Study. *Radiology* 287(1):224–234
21. Obmann MM, Kelsch V, Cosentino A, et al. (2019) Interscanner and Intrascanner Comparison of Virtual Unenhanced Attenuation Values Derived From Twin Beam Dual-Energy and Dual-Source. Dual-Energy Computed Tomography. *Invest Radiol*. 54(1):1–6
22. Helck A, Hummel N, Meinel FG, et al. (2014) Can single-phase dual-energy CT reliably identify adrenal adenomas? *Eur Radiol*. 24(7):1636–1642
23. Ananthakrishnan L, Rajiah P, Ahn R, et al. (2017 Mar) Spectral detector CT-derived virtual non-contrast images: comparison of attenuation values with unenhanced CT. *Abdom Radiol (NY)*. 42(3):702–709
24. Laukamp KR, Kessner R, Halliburton S, et al. Virtual Noncontrast Images From Portal Venous Phase Spectral-Detector CT Acquisitions for Adrenal Lesion Characterization. *J Comput Assist Tomogr*. 2020 Mar 11.

Publisher's Note Springer Nature remains neutral with regard to jurisdictional claims in published maps and institutional affiliations.